Asian Journal of Chemistry; Vol. 34, No. 8 (2022), 2025-2034

ASIAN JOURNAL OF CHEMISTRY

https://doi.org/10.14233/ajchem.2022.23677

Quantum Computational, Structural and Molecular Docking Analysis of 3,3,5,5-Tetramethyl-2-pyrrolidone: A DFT Approach

S. JEYAVIJAYAN[1,*], M. RAMUTHAI[1] and PALANI MURUGAN[2]

[1]Department of Physics, Kalasalingam Academy of Research and Education, Krishnankoil-626126, India
[2]Department of Physics, Dr. B.R. Ambedkar Institute of Technology, Port Blair-744103, Andaman & Nicobar Islands, India

*Corresponding author: E-mail: sjeyavijayan@gmail.com

Received: 14 December 2021; *Accepted*: 25 March 2022; *Published online*: 18 July 2022; AJC-20882

The work focused on 3,3,5,5-tetramethyl-2-pyrrolidone (TM-2-P) to be a potential candidate for breast cancer diagnosis based on density functional theory (DFT) and molecular docking calculations. The DFT used to predict the molecular geometries, molecular electrostatic potential and electronic properties with B3LYP/6-31+G(d,p) method. The geometrical parameters (bond angle and bond length) from DFT model are correlated with experimental values. The computed and experimental vibrational assignments have been determined by FT-IR and FT-Raman. To determine the charge transfer of molecule, the frontier orbital analysis has been utilized. The molecular interaction and chemical reactivity of the molecule are calculated by using the molecular electrostatic potential maps. The molecular docking calculation has been performed to obtain the biochemical activities of TM-2-P against the breast cancer studies.

Keywords: Density functional theory, 3,3,5,5-Tetramethyl-2-pyrrolidone, Frequency assignments, Molecular docking.

INTRODUCTION

The uncontrolled growth of abnormal cells in the body was due to some internal (inherited genetic mutation, immune conditions and hormones) and many external factors (radiation, chemical and viruses). The World Cancer Report-2008 stated the global cancer cases doubled in the last 30 years of the 20th century and it is expected that this will nearly triple by 2030. The cancer treatment and diagnosis carried out as per the following strategies such as chemotherapy, surgery, immune therapy, radiation, hormone therapy and targeted therapy [1]. Breast cancer is the second most common cancer overall and still the leading cancer-killer in women worldwide. The epidermal growth factor receptor (EGFR) is a receptor tyrosine kinase that is usually upregulated in cancers such as in metastatic colorectal cancer, non-small-cell lung cancer, glioblastoma, pancreatic cancer, head and neck cancer and breast cancer. For the triple negative breast cancer patient, EGFR is targeted as therapeutic intervention on its subgroup [2].

The pyrrolidine has five-membered ring with nitrogen widely used by medicinal purposes to cure human diseases. Recently, many studies provide to determine the suitable structure of pyrrolidone and its derivatives using the density functional theory (DFT) at B3LYP method [3,4]. From the literature data, no computation study has been done on 3,3,5,5-tetramethyl-2-pyrrolidone (TM-2-P) in the drug usage. In present work, the optimized structure of TM-2-P has been analyzed, which enables the potential breakthrough in the drug development based on molecular docking study. Also, the frontier orbital energies, Mullikan charges, intermolecular interactions of TM-2-P have been computed. The reactive nucleophilic and electrophilic regions of the molecule against the biological pathogens have been discussed by the molecular electrostatic potential surfaces. The molecular docking study is utilized effectively to find the efficient inhibitor for TM-2-P. The binding affinities and other different interactions that are associated between the various amino acid residues and ligands have been examined.

EXPERIMENTAL

Fourier transform infrared (FTIR) spectrum of 3,3,5,5-tetramethyl-2-pyrrolidone (TM-2-P) was recorded by Perkin-Elmer FTIR spectrometer employing a KBr pellet with a 1.0 cm^{-1} resolution. The FT-Raman spectrum of TM-2-P had taken

by using BRUKER RFS 27 model spectrometer with a resolution of 2 cm^{-1}. The FTIR and FT-Raman spectra were examined in the wavenumber range 4000-400 cm^{-1} and 4000-50 cm^{-1}, respectively.

Computational details: The GAUSSIAN 09W program [5] is used to achieve the DFT calculations and electronic properties of TM-2-P have been visualized by Gauss view 05 visualization [6] program. Initially, the structure is optimized by DFT/B3LYP/6-31+G(d,p) [7,8] and after that the wavenumbers, electronic properties are calculated. The scaled quantum mechanical (SQM) [9] method ensures the comparison between the experimental and DFT computed results. Hence, the calculated vibrations were scaled by value of 0.9613 for the B3LYP method [10]. The MOLVIB Program (Adaptation V7.0-G77) [11] by Sundius is performed to calculate the potential energy distribution (PED) for different vibrational modes. The UV-vis region of TM-2-P have been calculated (without any solvation) by using time-dependent (TD)-DFT/B3LYP method. The ^{13}C and ^{1}H NMR shielding was recorded using the Gauge-Invariant-atomic orbital (GIAO) method.

Protein and ligand structure: The main protein breast cancer, epidermal growth factor receptor [EGFR, PDB ID: 1AQC] is selected for the present study. The data for EGFR protein is found from the site (http://www.pdb.org) [12] and calculations are performed using the software discovery studio (version 2017 R2 client) [13]. The TM-2-P is considered as ligand and we found that it has good interaction with the EGFR protein. The details regarding the structure are taken from database PubChem (http://pubchem.ncbi.nlm.nih.gov)

Molecular docking: The molecular docking (MD) is executed by Auto Dock Vina (Adaptation: 4.2.1) [14] and MGL Apparatus 1.5.4. The hydrogen atoms are used to estimate the protonation of the given structure. The configuration file was generated using the box size coordinates and protein-ligand structure has been spared in pdbqt file format to calculate the binding affinities (Kcal/mol). The energy binding values for 10 various dockings for each ligand has been obtained. The Disclosure Studio 2017 R2 Client has been utilized to ensure the number of hydrogen bonds and non-covalent interactions for each composite.

RESULTS AND DISCUSSION

Molecular geometry analysis: The optimized structure of TM-2-P, which shows C_1 point symmetry is illustrated in Fig. 1. The bond angles and the bond lengths are calculated by the B3LYP method. The computed results along with the experimental X-ray [15] diffraction data is covered in Table-1. The calculated geometries are in good agreement with the observed values for TM-2-P. In the B3LYP/6-31+(d,p) calculation, the effect of coupling between the methyl groups and pyrrolidone ring can be understood from the rise in bond lengths of C3-C18, C3-C22, C5-C10, C5-C14 (1.546, 1.548, 1.546, 1.544 E by B3LYP and 1.547, 1.534, 1.545, 1.533 E by experimental). The computed ring bond lengths C1-N2, N2-C3, C3-C4, C4-C5 and C1-C5 are found as 1.401, 1.439, 1.401, 1.396 and 1.393 E, respectively (1.412, 1.472, 1.490, 1.387 and 1.375 E, by experimental). The C-H bonds would be affected by the impacts of inductive-mesomeric relations [16]. From the DFT calculations, the N2-C3-C22, C3-C4-C5, C1-C5-C14, C5-C1-N2 and N2-C1-O8 bond angles are computed as 109.68º, 107.18º, 109.91º, 109.93º and 130.11º (experimental values: 109.50º, 109.50º, 108.80º, 110.40º and 126.19º). The deviations in the bond lengths and bond angles explain the effect of substitutions such as methyl groups, nitrogen and oxygen atoms in the pyrrolidone ring. The optimized minimum energy calculated by the DFT-B3LYP method with lower basis set for TM-2-P is -443.93161292 Hartrees. The thermodynamic results of TM-2-P are reported in Table-2. When the interactions between the atoms in the molecule are very stronger, then the dipole moment will be high. Here, the computed dipole moment and total energy of TM-2-P are estimated as 4.271 Debye and 145.577 kcal mol^{-1}. The irrelevant vibrational energy (zero-point) is found (139.15703 kcal mol^{-1}) for TM-2-P. These thermodynamic limits can be used in the assessment of chemical responses of TM-2-P.

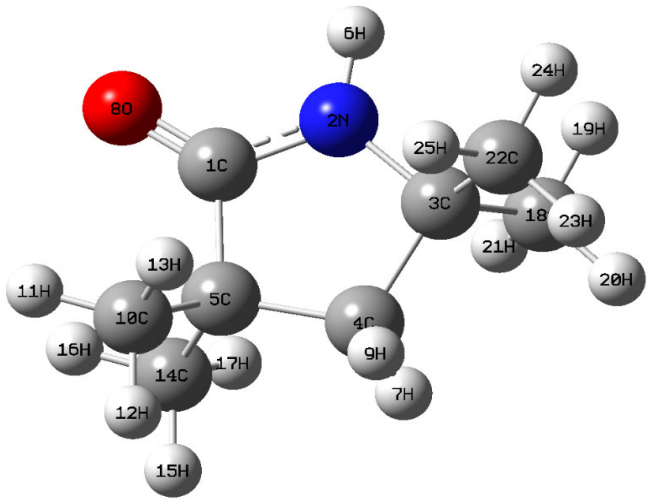

Fig. 1. Optimized structure of 3,3,5,5-tetramethyl-2-pyrrolidone

Vibrational assignments: TM-2-P contains 25 atoms and hence its 69 normal vibrations are active in the vibrational spectra (IR and Raman). The computed and experimental FTIR and FT-Raman spectra of TM-2-P are represented in Figs. 2 and 3. The peak intensities and the vibrational frequencies of TM-2-P are given in Table-3. N-H stretching [17] vibrations are found over the range from 3500-3000 cm^{-1} for heterocyclic compounds. Hence, the N-H vibrations are established at 3438 cm^{-1} (nearly 98% PED) in IR region as a weak band for TM-2-P. The N-H bending vibrations are well recognized by the literature results [18]. The C-H stretching vibrations [19] are built up in between 3100 and 3000 cm^{-1} and hence the computed frequencies at 3007 and 3003 cm^{-1} (nearly 95% PED) are assigned to C-H vibrations of TM-2-P. The corresponding experimental frequencies have been noted at 3088, 3078, 3022, 3014 cm^{-1} in both the vibrational spectra. In Table-3, the C-H bending vibrations of TM-2-P are also recorded. The C-N assignment vibrations are blended with several groups and distributed within the region 1382-1266 cm^{-1} for heteroaromatic compounds [20]. In TM-2-P, the band identified at 821, 814 in FTIR and 831, 821 cm^{-1} in FT-Raman spectra are given to the C-N stretching with 74% PED as illustrated in Table-3.

TABLE-1
OPTIMIZED GEOMETRICAL PARAMETERS OF 3,3,5,5-TETRAMETHYL-2-PYRROLIDONE

Bond length (Å)			Bond angles (°)			Dihedral angles (°)		
Parameters	B3LYP/6-31+G(d,p)	Experimental [15]	Parameters	B3LYP/6-31+G(d,p)	Experimental [15]	Parameters	B3LYP/6-31+G(d,p)	Experimental [15]
C1-N2	1.401	1.412	C4-C3-N2	108.41	107.79	N2-C3-C4-H7	-119.43	-119.93
C1-C5	1.393	1.375	C4-C3-C18	109.68	109.50	C18-C3-C4-H9	120.82	118.13
C3-C18	1.546	1.547	C4-C3-C22	109.68	109.50	C22-C3-C4-C5	119.74	129.32
C3-C22	1.548	1.534	N2-C3-C18	109.68	109.50	C4-C3-N2-H6	179.98	165.01
N2-C3	1.439	1.472	N2-C3-C22	109.68	109.50	C18-C3-2N-C1	119.74	129.32
C4-H7	1.070	0.969	C18-C3-C22	109.68	109.50	C18-C3-2N-H6	-60.27	-41.88
C4-H9	1.070	0.965	C3-C4-C5	107.18	109.50	C4-C3-C18-H19	-171.11	-179.05
C3-C4	1.401	1.490	C3-C4-C7	109.91	109.50	C4-C3-C18-H20	-51.11	-41.88
C5-C10	1.546	1.545	C3-C4-C9	109.91	109.50	C4-C3-C18-H21	68.88	78.99
C5-C14	1.544	1.533	C5-C4-C7	109.91	109.50	C4-C3-C22-H23	54.78	43.34
C4-C5	1.396	1.387	C7-C4-C9	109.91	109.50	N2-C3-C22-H24	53.74	42.16
C1-O8	1.468	1.488	C4-C5-C1	109.93	109.50			
N2-H6	0.981	0.971	C4-C5-C10	107.18	109.50			
C10-H11	1.073	0.962	C4-C5-C14	109.91	108.60			
C10-H12	1.073	0.962	C1-C5-C10	109.91	108.80			
C10-H13	1.073	0.962	C1-C5-C14	109.91	108.80			
C14-H15	1.073	0.962	C10-C5-C14	109.91	108.80			
C14-H16	1.073	0.962	C5-C1-N2	109.93	110.40			
C14-H17	1.073	0.962	C5-C1-O8	108.41	109.00			
C18-H19	1.073	0.962	N2-C1-O8	130.11	126.19			
C18-H20	1.073	0.962	C3-N2-C1	121.47	125.01			
C18-H21	1.073	0.962	C1-N2-C6	108.79	108.80			
C22-H23	1.073	0.962	C5-C10-H11	125.59	121.92			
C22-H24	1.073	0.962	C5-C10-H12	125.60	121.57			
C22-H25	1.073	0.962	C5-C10-H13	109.47	110.40			
			H11-C10-H12	109.47	109.50			
			H11-C10-H13	109.47	109.50			
			H12-C10-H13	109.47	109.50			
			C5-C14-H15	109.47	109.50			
			C5-C14-H16	109.47	109.50			
			C5-C14-H17	109.47	109.50			
			H15-C14-H16	109.47	109.50			
			H15-C14-H17	109.47	109.50			
			H16-C14-H17	109.47	109.50			
			C3-C18-H19	109.47	109.50			
			C3-C18-H20	109.47	111.19			
			C3-C18-H21	109.47	113.27			
			H19-C18-H20	109.47	109.50			
			H19-C18-H21	109.47	109.50			
			H20-C18-H21	109.47	109.50			
			C3-C22-H23	109.47	109.50			
			C3-C22-H24	109.47	113.55			
			C3-C22-H25	109.47	112.83			
			H23-C22-H24	109.47	112.68			
			H23-C22-H25	109.47	108.80			
			H24-C22-H25	109.47	108.80			

The C-C stretching vibrations play a vital part in the substituted aromatic framework. In general, the C-C frequencies are shown in the region 1624-726 cm^{-1} [21]. In TM-2-P, the experimental peaks at 1453, 1441, 1428, 1419, 1416, 1412, 1401 cm^{-1} in IR and 1458, 1431, 1425, 1421, 1417, 1411, 1404 cm^{-1} in Raman are attributed to C-C vibrations with 74-81% of PED. The corresponding DFT frequencies are obtained at 1520, 1512, 1510, 1506, 1503, 1496, 1493 cm^{-1}. The C=O vibrational [22] modes are generally observed in the wavenumber region 1780-1700 cm^{-1}. Therefore, the experimental C=O stretching mode of TM-2-P is observed at 1742 cm^{-1} in the FTIR and 1741 cm^{-1} in the FT-Raman spectrum. The scaled C=O mode is computed as 1707 cm^{-1} for TM-2-P.

Generally, the CH_3 in-plane stretching vibrations are found in the region between 2975 and 2840 cm^{-1} [19]. In repesent study, the calculated wavenumbers at 2999, 2997, 2986 and 2983 which fits with the experimental frequencies at 2998, 2951, 2944, 2939, 2991, 2956, 2942, 2932 cm^{-1} are assigned for methyl in-plane stretching vibrations (nearly 90% PED). Usually, the CH_3 distortions are found in between 1450-1400

TABLE-2
THERMODYNAMIC PARAMETERS FOR
3,3,5,5-TETRAMETHYL-2-PYRROLIDONE

Parameters	B3LYP/6-31+G(d.p)
Optimized global minimum energy (Hartrees)	-443.93161292
Total energy (thermal), E_{total} (kcal mol^{-1})	145.577
Heat capacity, C_v (cal mol^{-1} k^{-1})	40.971
Entropy, S (cal mol^{-1} k^{-1})	95.850
Total	
Translational	40.745
Rotational	29.479
Vibrational	25.626
Vibrational energy, E_{vib} (kcal mol^{-1})	143.799
Zeropoint vibrational energy (kcal mol^{-1})	139.15703
Rotational constants (GHz)	
A	1.95486
B	1.04337
C	0.96671
Dipole moment (Debye)	4.271

cm^{-1}. For TM-2-P, the CH_3 in-plane and out-of-plane bending vibrations are in good agreement with the previous literature [23]. The other methyl vibrations are also illustrated in Table-3.

Frontier molecular orbitals (FMOs), Electronic spectra and Mulliken's population analysis: The electronic energies are important for molecular interface, donor and acceptor electron orbitals and are represented as HOMO and LUMO [24]. The HOMO-LUMO of TM-2-P has been calculated with energy gap 6.2181eV, which reflects the chemical activity of TM-2-P. The major atomic orbital HOMO (E_{HOMO} = -9.6249 eV) represent the electron giver (nitrogen and oxygen atoms of pyrrolidone ring) and the LUMO (E_{LUMO} = -3.4068 eV) implies the leading electron acceptor (tetramethyl and C-C bond of ring). The energy separation of TM-2-P is displayed in Fig. 4. The other molecular properties such as global hardness, chemical potential and electrophilicity are also illustrated in Table-4. The data obtained for orbital energies shows the addition of tetramethyl in pyrrolidone ring strongly influences

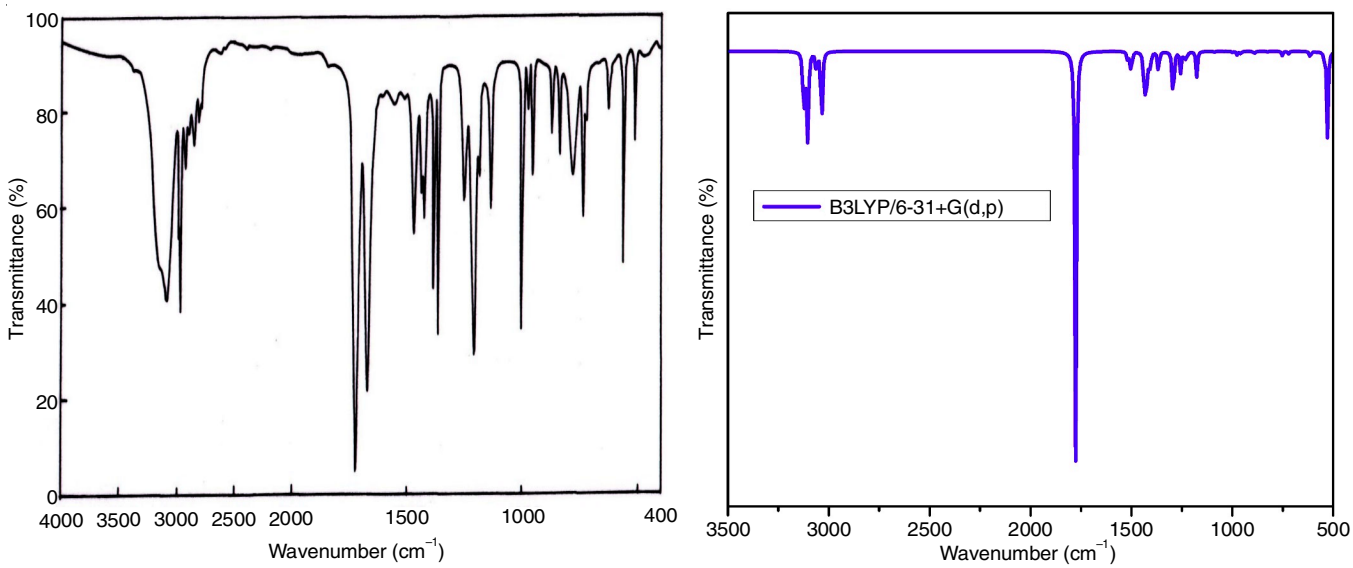

Fig. 2. FT-IR spectrum of 3,3,5,5-tetramethyl-2-pyrrolidone

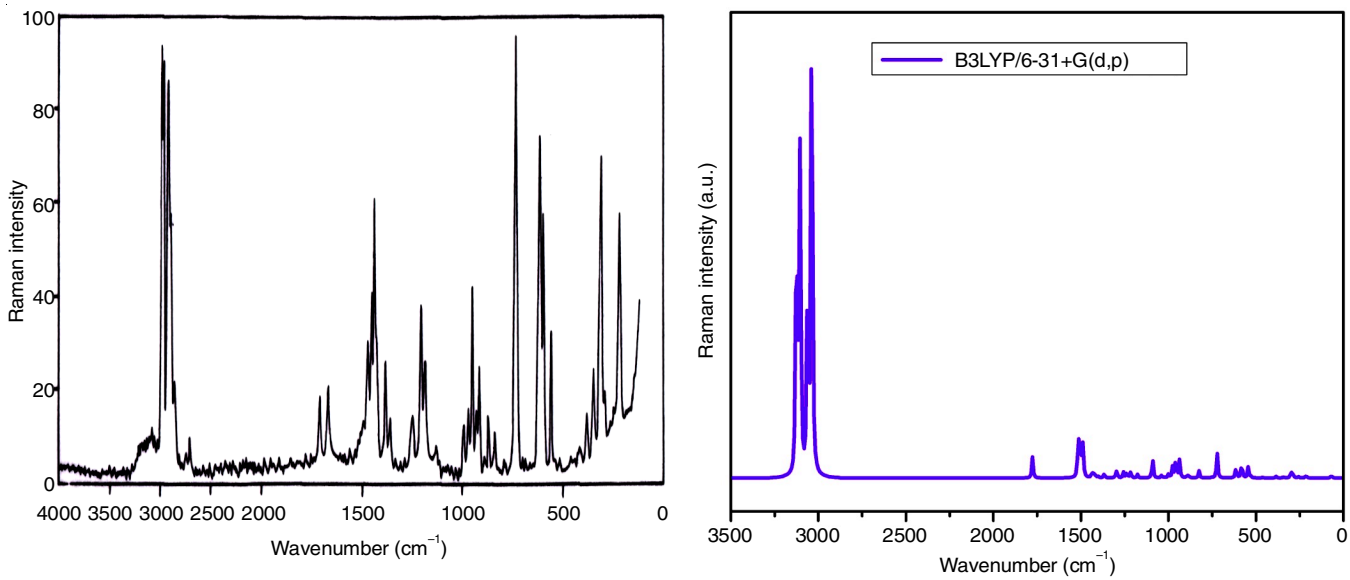

Fig. 3. FT-Raman spectrum of 3,3,5,5-tetramethyl-2-pyrrolidone

TABLE-3
CALCULATED VIBRATIONAL FREQUENCIES (cm^{-1}), IR INTENSITIES (Km mol^{-1}), RAMAN SCATTERING ACTIVITY ($Å^4$ amu^{-1}), REDUCED MASS (amu), FORCE CONSTANTS (mDyne/$Å^{-1}$) AND VIBRATIONAL ASSIGNMENTS BASED ON PED CALCULATIONS FOR 3,3,5,5-TETRAMETHYL-2-PYRROLIDONE

S. No.	Observed wavenumber		Wavenumber		IR intensity	Raman activity	Reduced mass	Force constant	Assignment with PED (%)
	FT-IR	FT-Raman	Calculated	Scaled					
1	3438(vw)	-	3620	3480	21.12	128.30	1.08	8.32	νNH(98)
2	3088(vw)	3078(w)	3128	3007	29.01	108.23	1.10	6.35	νCH(96)
3	3022(vw)	3014(w)	3124	3003	5.33	14.25	1.10	6.33	νCH(95)
4	2998(w)	2991(vs)	3120	2999	38.88	82.86	1.10	6.32	CH_3ips(92)
5	2951(vw)	2956(vs)	3117	2997	19.79	31.21	1.10	6.32	CH_3ips(91)
6	2944(vs)	2942(w)	3106	2986	52.67	144.02	1.10	6.26	CH_3ips(90)
7	2939(vs)	2932(w)	3103	2983	18.10	36.92	1.10	6.27	CH_3ips(89)
8	2903(vs)	2912(w)	3102	2982	47.55	89.39	1.10	6.25	CH_3ops(88)
9	2901(w)	2911(vw)	3100	2980	9.39	36.04	1.10	6.24	CH_3ops(90)
10	2899(w)	2903(vw)	3096	2977	1.41	5.31	1.10	6.24	CH_3ops(85)
11	2892(w)	2898(vw)	3061	2943	25.72	163.85	1.06	5.85	CH_3ops(86)
12	2879(vw)	2888(vw)	3037	2920	19.81	378.22	1.04	5.63	CH_3ass(84)
13	2877(vw)	2885(vw)	3036	2919	29.56	112.94	1.04	5.63	CH_3ass(85)
14	2873(vw)	2883(vw)	3033	2915	41.74	0.33	1.04	5.61	CH_3ass(82)
15	2871(vs)	2882(vw)	3031	2914	13.21	2.69	1.04	5.60	CH_3ass(81)
16	1742(vs)	1741(w)	1776	1707	501.06	11.72	9.76	18.13	?C=O(82)
17	1453(ms)	1458(vw)	1520	1461	8.62	5.09	1.06	1.45	νCC(80)
18	1441(ms)	1431(ms)	1512	1453	1.45	1.59	1.06	1.43	νCC(81)
19	1428(ms)	1425(vs)	1510	1451	0.26	19.70	1.08	1.45	νCC(79)
20	1419(ms)	1421(vs)	1506	1448	7.13	4.03	1.06	1.42	νCC(75)
21	1416(vs)	1417(vs)	1503	1445	13.87	2.98	1.08	1.43	νCC(78)
22	1412(vs)	1411(ms)	1496	1438	6.87	5.10	1.05	1.38	νCC(76)
23	1401(ms)	1404(ms)	1493	1435	1.34	0.38	1.05	1.38	νCC(74)
24	1396(ms)	1402(w)	1488	1431	0.35	14.01	1.05	1.36	CH_3ipb(70)
25	1391(ms)	1398(w)	1486	1428	0.01	3.22	1.05	1.36	CH_3ipb(74)
26	1342(w)	1334(w)	1435	1380	66.25	3.35	1.81	2.20	CH_3ipb(72)
27	1316(w)	1322(w)	1426	1371	25.92	0.52	1.26	1.51	CH_3ipb(71)
28	1317(ms)	1311(vw)	1420	1366	28.50	2.17	1.43	1.70	CH_3opb(69)
29	1312(ms)	1304(w)	1406	1351	20.68	0.10	1.25	1.45	CH_3opb(65)
30	1319(w)	1311(ms)	1402	1348	0.69	0.78	1.23	1.42	CH_3opb(66)
31	1311(ms)	1303(ms)	1365	1313	29.11	2.35	2.26	2.48	CH_3opb(68)
32	1208(ms)	1191(w)	1298	1248	2.12	2.62	1.62	1.60	CH_3sb(72)
33	1186(ms)	1181(w)	1293	1243	74.38	2.04	1.73	1.70	CH_3sb(70)
34	1241(vs)	1221(ms)	1256	1207	25.71	2.79	3.10	2.88	CH_3sb(72)
35	1213(vs)	1201(w)	1239	1191	4.35	2.07	2.49	2.25	CH_3sb(71)
36	1171(ms)	1161(w)	1229	1181	12.45	0.81	3.41	3.03	bNH(70)
37	1149(ms)	1141(w)	1215	1168	1.28	2.87	2.58	2.24	CH_3opr(67)
38	1002(ms)	1001(w)	1176	1131	31.16	1.70	1.98	1.61	CH_3opr(66)
39	998(ms)	998(ms)	1090	1048	1.24	9.86	1.53	1.07	CH_3opr(64)
40	994(ms)	994(ms)	1039	999	0.17	1.18	1.36	0.87	CH_3opr(65)
41	991(ms)	982(vs)	1022	982	0.19	0.22	1.29	0.79	CH_3ipr(72)
42	869(ms)	872(ms)	998	959	1.47	1.93	1.82	1.07	CH_3ipr(71)
43	853(ms)	849(ms)	975	938	4.63	5.14	1.87	1.05	CH_3ipr(70)
44	832(ms)	834(ms)	962	924	0.74	1.58	1.38	0.75	CH_3ipr(71)
45	821(ms)	831(ms)	957	920	2.87	7.92	2.08	1.12	νCN(74)
46	814(ms)	821(vs)	936	900	0.01	8.12	1.51	0.78	νCN(74)
47	816(ms)	819(vs)	891	857	3.59	1.56	2.09	0.98	bCH(71)
48	772(ms)	788(vw)	881	847	0.10	0.50	1.84	0.84	bCH(69)
49	769(ms)	778(vs)	824	793	0.70	3.19	3.93	1.57	ωCH(65)
50	741(w)	739(vs)	752	723	5.22	0.17	6.93	2.31	ωCH(64)
51	641(ms)	643(vs)	721	693	3.63	11.81	4.48	1.37	ωNH(62)
52	523(vs)	524(ms)	613	589	8.26	4.96	6.07	1.35	bCC (68)
53	519(ms)	512(ms)	580	558	0.99	7.11	3.09	0.61	bCC (70)
54	447(ms)	458(vs)	543	522	6.76	4.70	2.97	0.52	bCC (71)
55	441(ms)	451(ms)	528	507	104.55	0.55	1.18	0.19	bCC (70)
56	439(w)	449(ms)	461	443	0.03	0.30	2.59	0.33	bC=O(72)
57	418(w)	391(ms)	385	371	0.15	0.35	1.92	0.17	R_1asymd(67)

58	-	363(ms)	382	367	2.68	0.41	2.48	0.21	$R_i$symd(65)
59	-	301(ms)	341	328	0.31	0.45	2.13	0.15	t$R_i$symd(60)
60	-	298(ms)	300	289	0.98	1.55	2.05	0.11	t$R_i$asymd(62)
61	-	291(ms)	293	282	2.65	1.37	2.37	0.12	ωCC (65)
62	-	296(ms)	292	281	0.67	1.37	2.52	0.13	ωCC (64)
63	-	281(ms)	281	270	1.20	0.19	1.21	0.06	ωC=O(63)
64	-	266(s)	257	247	1.28	0.48	1.26	0.05	ωCC (64)
65	-	258(s)	251	242	0.00	0.06	1.04	0.04	ωCC (65)
66	-	211(s)	239	230	0.13	0.06	1.12	0.04	CH_{3twist} (59)
67	-	206(s)	213	204	0.14	1.05	2.44	0.06	CH_{3twist} (58)
68	-	161(s)	68	65	0.63	1.08	4.72	0.01	CH_{3twist} (59)
69	-	-	57	55	0.16	0.00	2.62	0.01	CH_{3twist} (58)

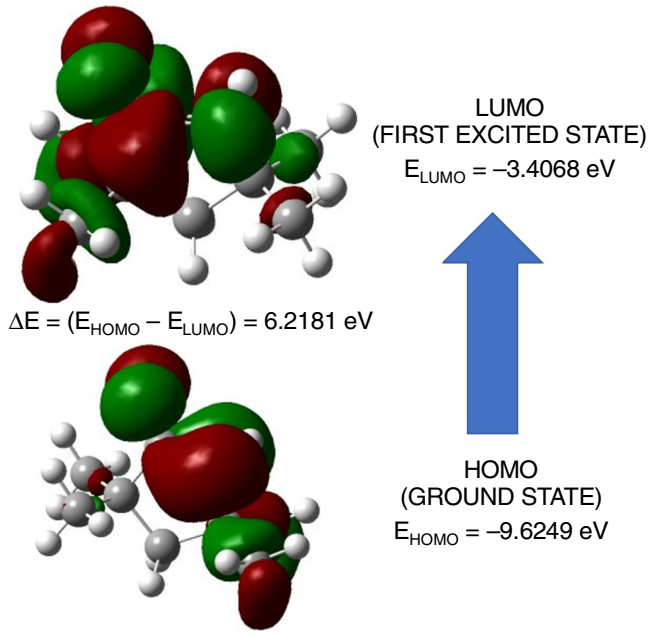

Fig. 4. HOMO-LUMO plot of 3,3,5,5-tetramethyl-2-pyrrolidone

TABLE-4
GLOBAL REACTIVITY DESCRIPTORS FOR
3,3,5,5-TETRAMETHYL-2-PYRROLIDONE

Molecular properties	B3LYP/6-31+G(d,p)
HOMO (eV)	-9.6249
LUMO (eV)	-3.4068
ΔE ($E_{HOMO} - E_{LUMO}$) (eV)	6.2181
Ionization potential (I)(eV)	9.6249
Electron affinity (A) (eV)	3.4068
Globalhardness (η) (eV)	3.1090
Global softness (s) (eV^{-1})	0.1608
Electronegativity (χ) (eV)	6.5158
Chemical potential (μ) (eV)	-6.5158
Global electrophilicity (ω) (eV)	6.8277

the energy gap because of high reactivity towards the molecule. Also, the lowering of energy gap makes the molecule softer so that it poses more reactive.

The frequency of oscillation (f), excitation energies (E) and electronic transitions of TM-2-P were computed by TD-DFT method [25]. A very strong peak is computed at 194.16 nm with energy E = 6.3632 eV and oscillator frequency of 0.0119 for TM-2-P. This corresponds to the transition from HOMO to LUMO (92% contribution), which belongs to π→π* type. The UV plot of TM-2-P is given in Fig. 5. Another energizing excitation computed at 193.24 nm with frequency f = 0.0082, E = 6.4160 eV from H-1→L (π→π* type) with contributions of 87% as listed in Table-5.

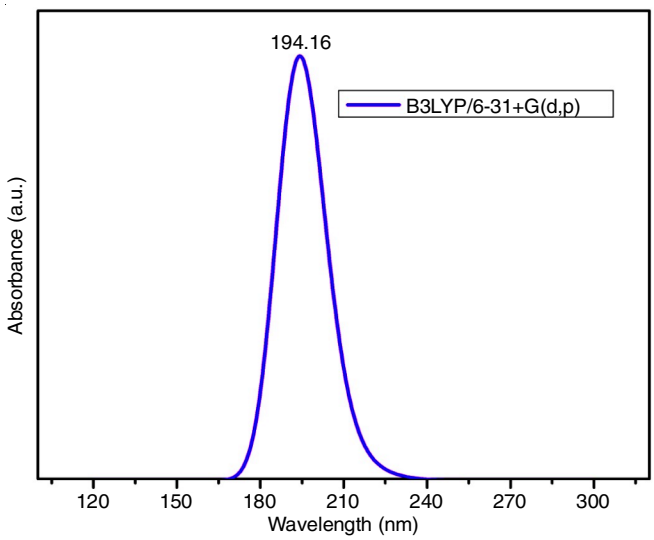

Fig. 5. UV plot of 3,3,5,5-tetramethyl-2-pyrrolidone

TABLE 5
MOLECULAR ORBITAL CONTRIBUTIONS OF
3,3,5,5-TETRAMETHYL-2-PYRROLIDONE

Energy (eV)	Oscillator strength	Wavelength (nm)	Major contributions	Assignment
6.3632	0.0119	194.16	H→L (92%)	π→π*
6.4160	0.0082	193.24	H-1→L (87%)	π→π*

Further, the reactive charges are computed by B3LYP with 6-31+G (d, p) basis set to provide the electronic properties of the molecule [26]. The Mulliken charge plot for TM-2-P is represented in Fig. 6 and values are given in Table-6. The positive values (0.306111, 0.152855, 0.152865, 0.176066, 0.146836, 0.147470, 0.146840, 0.176056, 0.147490, 0.144040, 0.152466, 0.158719, 0.152468, 0.144038 and 0.158716) of H6, H7, H9, H11, H12, H13, H15, H16, H17, H19, H20, H21, H23, H24 and H25 represents that TM-2-P is more acidic. The partial charges on C1, C3, C4, C5, C10, C14, C18 and C22 are highly influenced by their substituents. Further, due to lone pair electrons, the nitrogen and oxygen atoms N2 and O8 show the maximum negative charge for TM-2-P (-0.379225 and -0.501388).

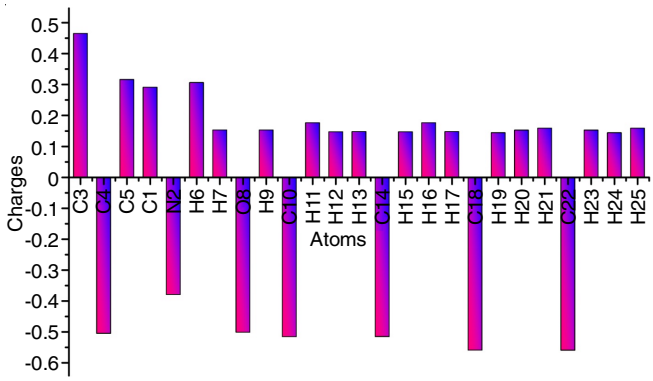

Fig. 6. Mulliken charges plot for 3,3,5,5-tetramethyl-2-pyrrolidone

TABLE-6
MULLIKEN ATOMIC CHARGE FOR
3,3,5,5-TETRAMETHYL-2-PYRROLIDONE

Atom	B3LYP/6-31+G(d.p)	Atom	B3LYP/6-31+G(d.p)
C1	0.290894	C14	-0.515309
N2	-0.379225	H15	0.146840
C3	0.464983	H16	0.176056
C4	-0.504714	H17	0.147490
C5	0.315829	C18	-0.559178
H6	0.306111	H19	0.144040
H7	0.152855	H20	0.152466
O8	-0.501388	H21	0.158719
H9	0.152865	C22	-0.559482
C10	-0.515445	H23	0.152468
H11	0.176066	H24	0.144038
H12	0.146836	H25	0.158716
H13	0.147470		

NMR studies: The ^{13}C and ^{1}H NMR spectra for TM-2-P had been utilized using the DFT/B3LYP/6-31+G (d,p) with GIAO method. This is the dynamic way to interpret the structure of enormous biomolecules. The chemical shift values have been computed with tetramethyl silane (TMS) as a reference and are illustrated in Table-7. The computed ^{13}C and ^{1}H NMR spectra have been shown in Fig. 7. In general, the chemical

TABLE-7
^{13}C AND ^{1}H NMR CHEMICAL SHIFTS FOR
3,3,5,5-TETRAMETHYL-2-PYRROLIDONE

^{13}C Assignment	Calculated shift (ppm)	^{1}H Assignment	Calculated shift (ppm)
C1	165.58	H6	5.14
C3	46.17	H7	2.21
C4	41.35	H9	2.20
C5	36.04	H20	1.49
C22	21.52	H23	1.48
C18	21.53	H25	1.47
C14	18.66	H21	1.46
C10	18.64	H16	1.45
		H11	1.44
		H19	1.43
		H24	1.42
		H13	1.37
		H17	1.36
		H15	1.30
		H12	1.29

shifts of aromatic carbons lie between 100 to 200 ppm [27]. In this case, the computational ^{13}C NMR shifts are gotten from 165.58 to 18.64 ppm. Here, the high electronegative properties of nitrogen atom deliver positive charges to the carbon atoms. Hence, the highest shift is obtained for C1 and C3 (165.58 and 46.17 ppm). The carbon atoms C10, C14, C18 and C22 give the lowest shift at 18.64, 18.66, 21.53 and 21.52 ppm, respectively, since they are attached with the H-atoms of methyl groups. The hydrogen atoms coupled with methyl groups shows the lowest shift ranges between 1.29 and 1.49 ppm. The calculated chemical shifts for H6, H7 and H9 attached directly to nitrogen and ring carbon atoms have the maximum value of 5.14, 2.21 and 2.20 ppm, respectively.

Molecular electrostatic potential (MEP) surface analysis: MEP surface has been calculated to get the responsive locales of electrophilic, nucleophilic regions of the molecule. Moreover, the MEP plot is used to differentiate the electron deficient, slightly deficient, rich, slightly rich by using its colour codes as blue colour, light blue colour, red and yellow,

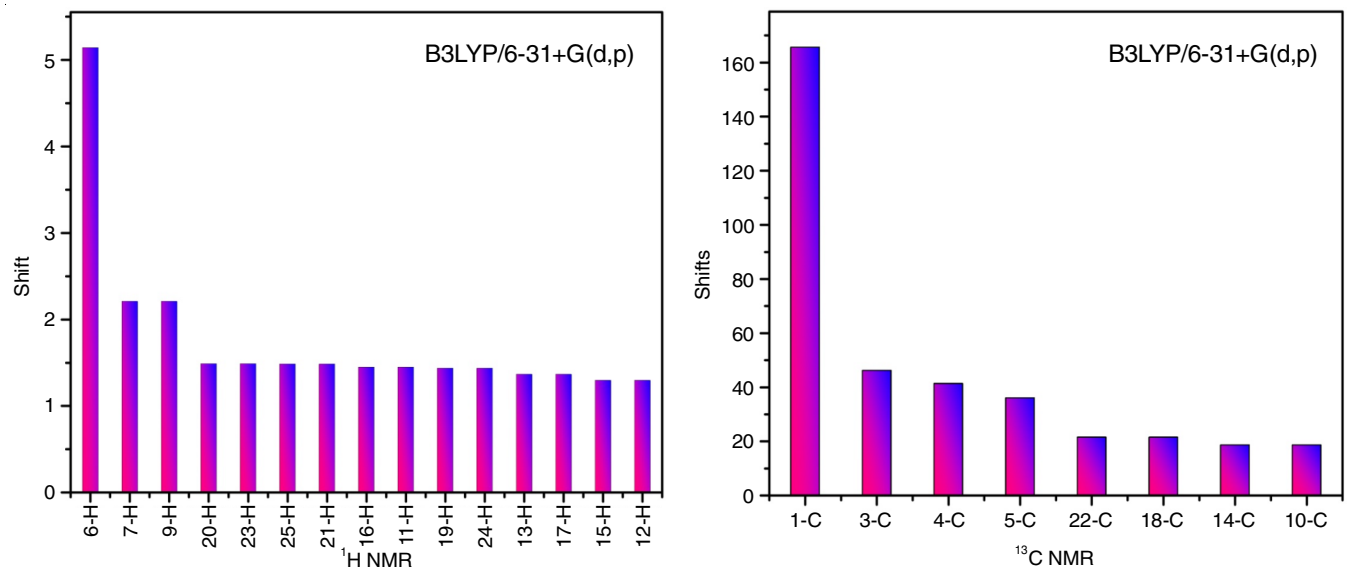

Fig. 7. ^{1}H and ^{13}C NMR theoretical spectra for 3,3,5,5-tetramethyl-2-pyrrolidone

respectively [28]. In the MEP plot, the positive potential site is more favourable to nucleophilic attack and on the other hand the negative potential sites are responsible for the electrophilic attack. The MEP image of TM-2-P has been portrayed in Fig. 8. The negative potential sites of TM-2-P are accumulated near to oxygen atom (red region) of the molecule. The nucleophilic regions are found close to all the hydrogens (blue region) especially hydrogen attached with nitrogen (H6). Hence, the hydrogen and oxygen atoms of TM-2-P has secured to be most attractive and repulsion regions, respectively.

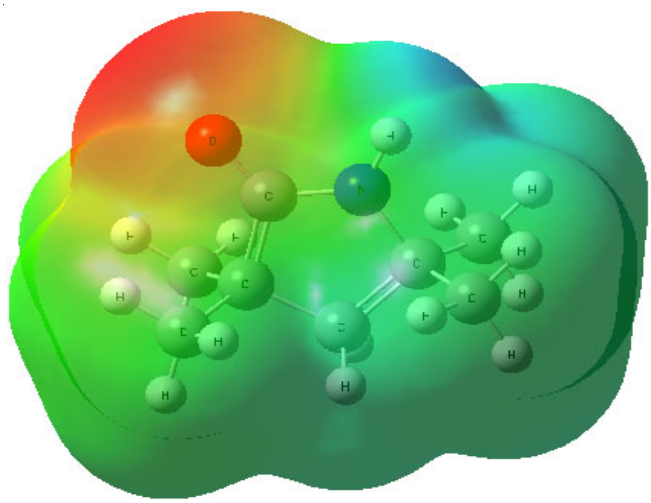

Fig. 8. MEP plot of 3,3,5,5-tetramethyl-2-pyrrolidone

Natural bond orbital (NBO) analysis: To measure the intermolecular and intramolecular interactions, NBO analysis has been utilized [29]. This clarifies the donor–acceptor relations using second-order Fock matrix and the computed results are detailed in Table-8. In general, greater the stabilization energy will lead more tendency to donate(i) electrons to acceptor(j) orbitals and is expected as:

$$E_2 = \Delta E_{ij} = q_i \frac{F(i,j)^2}{\varepsilon_i - \varepsilon_j}$$

where F(i,j) is the Fock matrix element, ε_i and ε_j represents diagonal elements and q_i is the donor orbital occupancy. The intramolecular charge transfer (ICT) conjugation from σ to σ* is the distinctive feature for medicinal uses of the molecule [30]. In TM-2-P, the greater intramolecular energy obtained between the LP(N2) and π*(C1-O8) orbitals with stabilization of 68.49 kcal mol^{-1}. The n-σ interaction among the oxygen, lone pair of electrons in nitrogen and π-π* interaction in the pyrrolidone ring are very tough in the ground state. These explain the more bioactive nature of the molecule and are stabilized by these interactions.

Molecular docking: Epidermal growth factor receptor (EGFR) is a tyrosine kinase receptor upregulated in breast cancer. It is involved in the cell growth, cell survival and metastasis [31]. Molecular docking studies have been revealed that the TM-2-P interacts with the breast cancer marker protein (EGFR). The binding energies and interacting residues are illustrated

TABLE-8
SECOND-ORDER PERTURBATION THEORY STUDY OF FOCK MATRIX FOR 3,3,5,5-TETRAMETHYL-2-PYRROLIDONE BY NBO ANALYSIS

Donor(i)	ED(i) (e)	Acceptor (j)	ED (j) (e)	Stabilization energy E(2) (kcal mol^{-1})	Energy difference E(j) – E(i) (a.u.)	Fock matrix element F (I,j) (a.u.)
σ(C1-C2)	1.97176	σ*(N2-H6)	0.02081	3.6	1.03	0.054
σ(C1-N2)	1.98228	σ*(C4-O8)	0.01211	4.22	1.34	0.067
σ(C2-C3)	1.97384	σ*(C4-O8)	0.01211	4.24	1.19	0.064
σ(C3-C4)	1.96407	σ*(N2-H6)	0.02081	3.94	1.05	0.058
σ(C3-C14)	1.97259	π*(C4-O8)	0.29315	2.47	0.61	0.037
σ(N2-H6)	1.98782	σ*(C3-C4)	0.08304	2.76	1.04	0.049
σ(C10-H11)	1.98849	σ*(C2-C3)	0.02236	3.39	0.85	0.048
σ(C10-H12)	1.98840	σ*(C3-C4)	0.08304	2.55	0.87	0.043
σ(C10-H13)	1.98961	σ*(C3-C14)	0.01793	3.04	0.87	0.046
σ(C14-H15)	1.98840	σ*(C3-C4)	0.08304	2.55	0.87	0.043
σ(C14-H16)	1.98849	σ*(C2-C3)	0.02236	3.39	0.85	0.048
σ(C14-H17)	1.98961	σ*(C3-C10)	0.01793	3.04	0.87	0.046
σ(C18-H19)	1.98909	σ*(C1-C2)	0.02667	3.24	0.84	0.047
σ(C18-H20)	1.98652	σ*(C1-N2)	0.03739	4.01	0.85	0.052
σ(C18-H21)	1.98909	σ*(C1-C22)	0.02644	3.11	0.86	0.046
σ(C22-H23)	1.98652	σ*(C1-N2)	0.03739	4.01	0.85	0.052
σ(C22-H24)	1.98909	σ*(C1-C2)	0.02667	3.24	0.84	0.047
σ(C22-H25)	1.98909	σ*(C1-C18)	0.02642	3.11	0.86	0.046
LP(N2)	1.69428	σ*(C1-C18)	0.02642	5.07	0.61	0.053
LP(N2)	1.69428	σ*(C1-C22)	0.02644	5.08	0.61	0.053
LP(N2)	1.69428	π*(C1-O8)	0.29315	68.49	0.28	0.123
LP(O8)	1.97606	σ*(C3-C4)	0.08304	2.44	1.04	0.046
LP(O8)	1.97606	σ*(C4-N5)	0.07476	2.38	1.16	0.047
LP2(O8)	1.85909	σ*(C3-C4)	0.08304	21.02	0.61	0.103
LP2(O8)	1.85909	σ*(C1-N2)	0.07476	25.97	0.72	0.124

TABLE-9a
DOCKING CALCULATION SHOWING FOR 3,3,5,5-TETRAMETHYL-2-PYRROLIDONE INTERACTING RESIDUES AND ATOMS INVOLVED IN H-BONDING

Protein	Interacted Residues	Ligand and Protein atom involved in H-bonding
(EGFR) (PDB ID: 1AQC)	PRO A:7, CYS A:6, TYR A:3, GLY A:5	CYS A:6

TABLE-9b
MOLECULAR DOCKING RESULTS FOR 3,3,5,5-TETRAMETHYL-2-PYRROLIDONE WITH EGFR

Protein	Binding energy	Ligand efficiency	Inhibit constant	Intermol energy	vdw HB dissolve energy	Electrostatic energy	Total internal	Torsional energy	Unbound energy
(EGFR) (PDB ID: 1AQC)	-4.80	-0.86	47.44	-4.14	-4.06	-0.03	-0.02	0.4	-0.02

in Tables 9a and 9b, respectively. Present docking results between TM-2-P and EGFR revealed that the TM-2-P make a hydrophobic interaction with PRO A:7, CYS A:6, TYR A:3 and GLY A:5 (Fig. 9). The inhibition activity of EGFR has the highest binding energy with TM-2-P and is observed as -4.80 Kcal mol^{-1}. Therefore, it is sensible to speculate that the studied molecule TM-2-P might have effective breast cancer activity.

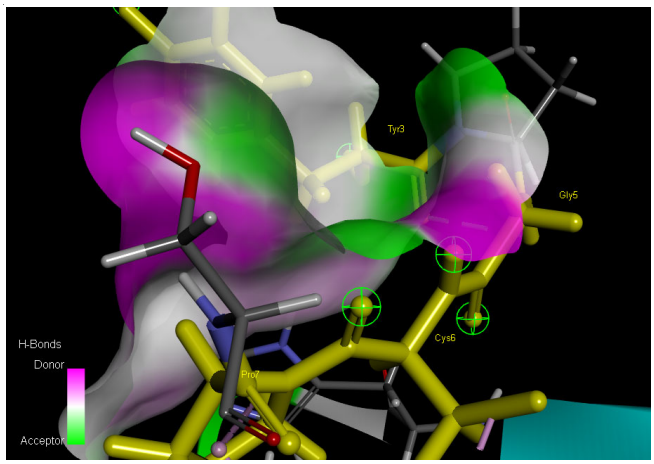

Fig. 9. 3,3,5,5-Tetramethyl-2-pyrrolidone interacts with the (EGFR) (PDB ID: 1AQC) protein

Conclusion

The geometrical and vibrational properties of 3,3,5,5-tetramethyl-2-pyrrolidone have been examined by B3LYP-6-31+G(d,p) method. Computed frequencies of normal modes show well agreement with the experimental values. MEP describes the electrophilic (oxygen) and nucleophilic (hydrogen) responsive locales of the molecule. The Mulliken charge distribution and FMO analysis confirm the chemical properties of the molecule. The electronic spectra of the molecule have been performed which reflects the results of FMOs. The computed carbon and proton shift reflects the detailed structural information and the NBO outcome indicates the intra and intermolecular charge exchange of the molecule. Furthermore, it is found that the molecular docking study plays an important role in the binding of a ligand molecule with the breast cancer marker protein EGFR, which could be a target for future study. These results indicate that the TM-2-P might have potential drug in the pharmaceuticals and biomedicines.

CONFLICT OF INTEREST

The authors declare that there is no conflict of interests regarding the publication of this article.

REFERENCES

1. Y.H. Xie, Y.X. Chen and J.Y. Fang, *Sig. Transduct. Target Ther.*, **5**, 22 (2020); https://doi.org/10.1038/s41392-020-0116-z
2. R.C. DeConti, *Semin. Oncol.*, **39**, 145 (2012); https://doi.org/10.1053/j.seminoncol.2012.01.002
3. S.O. Souza, R.B. Lira, C.R.A. Cunha, B.S. Santos, A. Fontes and G. Pereira, *Top. Curr. Chem.*, **379**, 1 (2021); https://doi.org/10.1007/s41061-020-00313-7
4. M.E. Vaschetto, B.A. Retamal and A.P. Monkman, *J. Mol. Struct. THEOCHEM*, **468**, 209 (1999); https://doi.org/10.1016/S0166-1280(98)00624-1
5. M.J. Frisch, G.W. Trucks, H.B. Schlegal, G.E. Scuseria, M.A. Robb, J.R. Cheesman, V.G. Zakrzewski, J.A. Montgomerg Jr., R.E. Stratmann, J.C. Burant, S. Dapprich, J.M. Millam, A.D. Daniels, K.N. Kudin, M.C. Strain, O. Farkas, J. Tomasi, V. Barone, M. Cossi, R. Cammi, B. Mennucci, C. Pomelli, C. Adamo, S. Clifford, J. Ochterski, G.A. Petersson, P.Y. Ayala, Q. Cui, K. Morokuma, N. Rega, P. Salvador, J.J. Dannenberg, D.K. Malich, A.D. Rabuck, K. Raghavachari, J.B. Foresman, J. Cioslowski, J.V. Ortiz, A.G. Baboul, B.B. Stetanov, G. Liu, A. Liashenko, P. Piskorz, I. Komaromi, R. Gomperts, R.L. Martin, D.J. Fox, T. Keith, M.A. Al-Laham, C.Y. Peng, A. Nanayakkara, M. Challacombe, P.M.W. Gill, B. Johnson, W. Chen, M.W. Wong, J.L. Andres, C. Gonzalez, M. Head-Gordon, E.S. Replogle and J.A. Pople, GAUSSIAN 09, Revision A 11.4, Gaussian, Inc, Pittsburgh, PA (2009).
6. T. Keith and J. Milam, Gauss View, Semichem Inc.; Shawnee Mission KS version 5, Ray Dennington (2009).
7. A.D. Becke, *J. Chem. Phys.*, **98**, 5648 (1993); https://doi.org/10.1063/1.464913
8. C. Lee, W. Yang and R.G. Parr, *Phys. Rev.*, **37**, 785 (1988); https://doi.org/10.1103/PhysRevB.37.785
9. M. Castellà-Ventura, E. Kassab, G. Buntinx and O. Poizat, *Phys. Chem. Chem. Phys.*, **2**, 4682 (2000); https://doi.org/10.1039/B006459I
10. D.C. Young, Computational Chemistry: A Practical Guide for Applying Techniques to Real World Problems (Electronic), John Wiley & Sons Ltd.: New York (2001).
11. MOLVIB (V.7.0), Calculation of Harmonic Force Fields and Vibrational Modes of Molecules, QCPE Program No. 807 (2002).
12. U.P. Mohan, S. Kunjiappan, P.B.T. Pichiah and S. Arunachalam, *3 Biotech.*, **11**, 15 (2021); https://doi.org/10.1007/s13205-020-02530-9
13. B.L. Narayana, D.P. Kishore, C. Balakumar, K.V. Rao, R. Kaur, A.R. Rao, J. Murthy and M. Ravikumar, *Chem. Biol. Drug Des.*, **79**, 674 (2012); https://doi.org/10.1111/j.1747-0285.2011.01277.x
14. O. Trott and A.J. Olson, *J. Comput. Chem.*, **31**, 455 (2009); https://doi.org/10.1002/jcc.21334

15. Y.P. Liu, X.F. Zhang, K.J. Liu and Y. Liu, *Acta Crystallogr. Sect. E Struct. Rep. Online*, **62**, o3672 (2006); https://doi.org/10.1107/S1600536806029849
16. M.K. Ahmed and B.R. Henry, *J. Phys. Chem.*, **90**, 1737 (1986); https://doi.org/10.1021/j100400a002
17. N.L. John, S. Abraham, D. Sajan, B.K. Sarojini and B. Narayana, *J. Mol. Struct.*, **1222**, 128939 (2020); https://doi.org/10.1016/j.molstruc.2020.128939
18. V. Krishnakumar and R.J. Xavier, *Spectrochim. Acta A Mol. Biomol. Spectrosc.*, **60**, 709 (2004); https://doi.org/10.1016/S1386-1425(03)00281-6
19. V. Siva, S.S. Kumar, M. Suresh, M. Raja, S. Athimoolam and S.A. Bahadur, *J. Mol. Struct.*, **1133**, 163 (2017); https://doi.org/10.1016/j.molstruc.2016.11.088
20. M. Arivazhagan, S. Jeyavijayan and J. Geethapriya, *Spectrochim. Acta A Mol. Biomol. Spectrosc.*, **104**, 14 (2013); https://doi.org/10.1016/j.saa.2012.11.032
21. G. Sivaraj, N. Jayamani and V. Siva, *J. Mol. Struct.*, **1240**, 130530 (2021); https://doi.org/10.1016/j.molstruc.2021.130530
22. Y. Erdogdu, *Spectrochim. Acta A Mol. Biomol. Spectrosc.*, **106**, 25 (2013); https://doi.org/10.1016/j.saa.2012.12.043
23. A. Regiec and P. Wojciechowski, *J. Mol. Struct.*, **1196**, 370 (2019); https://doi.org/10.1016/j.molstruc.2019.06.028
24. S. Jeyavijayan, M. Ramuthai and P. Murugan, *Asian J. Chem.*, **33**, 2313 (2021); https://doi.org/10.14233/ajchem.2021.23308
25. S. Jeyavijayan and P. Murugan, *Asian J. Chem.*, **33**, 83 (2020); https://doi.org/10.14233/ajchem.2021.22922
26. B. Pramodh, P. Naresh, S. Naveen, N.K. Loganth, S. Ganguly, J. Panda, S. Murugesan, A.V. Raghu and I. Warad, *Chem. Data Coll.*, **31**, 100587 (2021); https://doi.org/10.1016/j.cdc.2020.100587
27. K. Rastogi, M.A. Palafox, R.P. Tanwar and L. Mittal, *Spectrochim. Acta A Mol. Biomol. Spectrosc.*, **58**, 1987 (2002); https://doi.org/10.1016/S1386-1425(01)00650-3
28. O. Noureddine, N. Issaoui, M. Medimagh, O. Al-Dossary and H. Marouani, *J. King Saud Univ. Sci.*, **33**, 101334 (2021); https://doi.org/10.1016/j.jksus.2020.101334
29. M. Nsangou, Z. Dhaouadi, N. Jaïdane and Z. Ben Lakhdar, *J. Mol. Struct. THEOCHEM*, **819**, 142 (2007); https://doi.org/10.1016/j.theochem.2007.05.038
30. S.P.V. Chamundeeswari, E.J.J. Samuel and N. Sundaraganesan, *Mol. Simul.*, **38**, 987 (2012); https://doi.org/10.1080/08927022.2012.682279
31. M.G. Sugiyama, G.D. Fairn and C.N. Antonescu, *FASEB J.*, **34(S1)**, 1 (2020); https://doi.org/10.1096/fasebj.2020.34.s1.05687